complex does, the true cause is not apparent. Thus, at present the major factor in the determination of the association constants and the temperature variation of the CD intensity of the ion pair is not clear.

DCD Spectra. As shown in Figure 2, all the DCD spectra due to both *d*- and *l*-tartrates, except for Δ-[Co(sen)]$^{3+}$···*d*-tartrate, are composed of apparently single peaks. The DCD's of the en, 1-pn, and 1-chxn complexes are all positive, whereas they are negative for Δ-[Co(sep)]$^{3+}$···*d*- and *l*-tartrates. If we note that the tartrate anion approaches the former four complexes predominantly along the C_3 axis and the anion approaches Δ-[Co(sep)]$^{3+}$ mainly along the C_2 axis and that $R(A_2)$ and $R(E_a)$ are positive and negative, respectively, for all the complexes, this observation seems to support the idea that an access of an anion along the C_3 axis enhances $R(A_2)$ and that along the C_2 axis enhances $R(E_a)$.[6,28] It may be apparent that the observed DCD is a compromise of two opposing effects: enhancement of $R(A_2)$, which is positive, due to the C_3 access of the anion and enhancement of $R(E_a)$, which is negative, due to the C_2 access. The sign of the observed DCD reflects the dominant mode of these two. The small negative peak observed in the DCD of Δ-[Co(sen)]$^{3+}$···*d*-tartrate is thus assigned to E_a, and the dominant peak is therefore assigned to A_2. From comparison of the DCD spectra in Figure 2 except that of Δ-[Co(sep)]$^{3+}$, it is apparent

that the positive DCD's are assigned to A_2.

The CD curves of fully ion-paired species are also given in Figure 2. As seen from the figure, the CD spectra of Δ-[Co(en)$_3$]$^{3+}$, Δ-*fac*- and Δ-*mer*-[Co(1-pn)$_3$]$^{3+}$, and Δ-[Co(1-chxn)$_3$]$^{3+}$ tend to be close to the CD of Δ-[Co(sen)]$^{3+}$ upon ion pairing. The CD spectrum of Δ-[Co(sep)]$^{3+}$ tends, upon ion pairing, to mimic the CD spectrum of the ion pair formed between Δ-*fac*- or Δ-*mer*-[Co(1-pn)$_3$]$^{3+}$ or Δ-[Co(1-chxn)$_3$]$^{3+}$ and *d*- or *l*-tartrate. These observations are consistent with the conclusion of Mason et al.[28] that the addition of atoms or groups, whether covalent or hydrogen bonded, to the D_3 polar region of trigonal [Co(N)$_6$]$^{3+}$ complexes enhances generally $R(A_2)$ and that to the D_3 equatorial region enhances $R(E_a)$. Finally, it will be worthwhile to point out that the intensity and the shape of a CD spectrum change, in some complexes, rather drastically by ion pairing. For example, the CD peak of Δ-[Co(sep)]$^{3+}$ diminishes in intensity by about 64% and the shape also changes as illustrated in Figure 2, due to tartrates. A direct consequence of this is that the intensity as well as the shape of the CD spectra taken especially for single crystals is more or less modified by "ion pairing" effects in the solid state.

Registry No. Δ-[Co(en)$_3$]$^{3+}$, 16569-46-3; Δ-[Co(sen)]$^{3+}$, 85353-30-6; Δ-[Co(sep)]$^{3+}$, 85283-43-8; Δ-*fac*-[Co(1-pn)$_3$]$^{3+}$, 18745-20-5; Δ-*mer*-[Co(1-pn)$_3$]$^{3+}$, 36513-61-8; Δ-[Co(1-chxn)$_3$]$^{3+}$, 60064-15-5; *d*-tartrate, 3715-17-1; *l*-tartrate, 5976-86-3.

(28) Drake, A. F.; Kuroda, R.; Mason, S. F. *J. Chem. Soc., Dalton Trans.* **1979**, 1095.

Contribution from the Department of Chemistry, Massachusetts Institute of Technology, Cambridge, Massachusetts 02139

# Photoassisted Reduction of Sulfur Dioxide in Nonaqueous Solutions at p-Type Semiconductor Electrodes

GARY S. CALABRESE, TED J. SOBIERALSKI, and MARK S. WRIGHTON*

The electrochemical behavior of SO$_2$ has been investigated at illuminated (632.8 and 514.5 nm) p-type semiconducting Si, WS$_2$, and InP in CH$_3$CN/[*n*-Bu$_4$N]ClO$_4$ solutions. SO$_2$ is photoreducible at each of these materials to form S$_2$O$_4^{2-}$, but the electrical power savings efficiencies are variable. The best power savings efficiency, ~11% at 514.5 nm (100 mW/cm^2), is obtained with a p-type InP photocathode modified by photoelectrodeposition of ~5 × 10^{-8} mol/cm^2 of Pt onto the surface. Naked p-InP is considerably less efficient, owing to poor kinetics for the reduction of SO$_2$. The deposition of Pt onto p-InP forms neither a uniform ohmic contact nor a Schottky barrier; rather, studies of platinized n-InP show directly that the Pt serves as a catalyst for SO$_2$ reduction. Power savings efficiencies for p-type WS$_2$ and textured Si are low, owing to small output voltages. Preparative, controlled-potential photoelectrochemical reduction of SO$_2$ at all three photoelectrodes and Pt in CH$_3$CN/0.1 M SO$_2$/0.5 M [*n*-Bu$_4$N]ClO$_4$ has been demonstrated to give >90% current efficiency for formation of S$_2$O$_4^{2-}$, which can be precipitated and collected as Na$_2$S$_2$O$_4$.

Introduction

There is much interest in demonstrating worthwhile redox reactions that can be driven by illumination of semiconductors immersed in liquid electrolytes.[1] Recently,[2] we showed that the uphill reduction of 2-*tert*-butyl-9,10-anthraquinone in CH$_3$CN/CH$_3$COOH/electrolyte solution can be sustained at p-type Si photocathodes and that exposure of the electrolyzed solutions to O$_2$ results in the formation of synthetically significant quantities of H$_2$O$_2$. With the goal of demonstrating a photoelectrochemical route to the known reductant S$_2$O$_4^{2-}$, we have undertaken a study of the electrolysis of nonaqueous solutions of SO$_2$ using p-type WS$_2$, Si, and InP photocathodes (eq 1). The light-assisted reduction of SO$_2$ according to eq

$$2SO_2 + 2e^- \xrightarrow[\text{nonaqueous electrolyte}]{\text{p-type photocathode, } 2h\nu} S_2O_4^{2-} \qquad (1)$$
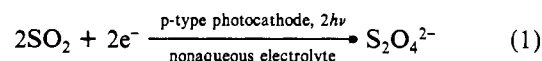
1 is shown to occur at electrode potentials more positive than that when the reduction is carried out at conventional electrodes such as Pt, thereby lowering the electrical energy required for S$_2$O$_4^{2-}$ generation.

The reduction of SO$_2$ to S$_2$O$_4^{2-}$ is irreversible in the kinetic sense,[3] and complicated electrolyte and SO$_2$ concentration dependent equilibria make $E^{\circ\prime}$(SO$_2$/S$_2$O$_4^{2-}$) difficult to de-

(1) Bard, A. J. *Science (Washington, D.C.)* **1980**, *207*, 139.
(2) Calabrese, G. S.; Wrighton, M. S. *J. Electrochem. Soc.* **1981**, *128*, 1014.

(3) (a) Martin, R. P.; Sawyer, D. T. *Inorg. Chem.* **1972**, *11*, 2644. (b) Mango, F.; Mazzocchin, G. A.; Bontempelli, G. *J. Electroanal. Chem. Interfacial Electrochem.* **1974**, *57*, 89. (c) Gardner, C. L.; Fouchard, D. T.; Fawcett, W. R. *J. Electrochem. Soc.* **1981**, *128*, 2337. (d) Gardner, C. L.; Fouchard, D. T.; Fawcett, W. R. *Ibid.* **1981**, *128*, 2345. (e) Bruno, P.; Caselli, M.; Traini, A. *J. Electroanal. Chem. Interfacial Electrochem.* **1980**, *113*, 99.
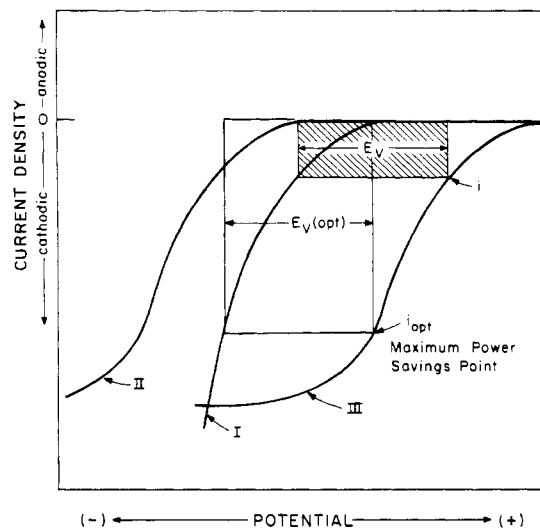
Figure 1. Representation of current–voltage curves for a cathodic process at a conventional electrode (curve I), at a photocathode that does not lead to power savings (curve II), and at a photocathode that does yield significant power savings (curve III). For the photocathode associated with curve II the efficiency, η (cf. eq 1 in text), is negative, meaning that compared to the case for the conventional electrode more electrical energy *and* optical energy are required to effect the cathodic process at a given current density, since the process occurs more negative at all current densities at the photocathode. The photocathode characterized by curve III does yield power savings since the process can be effected at more positive electrode potentials at the illuminated electrode. For discussion of the efficiency, see text.

termine.[3d] These problems complicate discussion of the efficiency for converting incident light to useful energy. We choose to define efficiency, η in percent, according to eq 2,

$$\eta = \frac{\text{electrical power saved}}{\text{incident optical power}} \times 100\% \qquad (2)$$

where electrical power saved refers to the power saved by using a photocathode-based cell compared to a conventional cathode-based cell operated at the same cathodic current density. In many instances the power saved will be a function of the photocathode *and* the conventional cathode.[4] It is obvious why the efficiency would be dependent on the properties of the photocathode. However, the efficiency according to eq 2 could vary with the conventional cathodes too, since the overvoltage for a given electrochemical process depends on the electrode.[5] In this study we have used Pt as the conventional cathode material in determinations of energy conversion efficiency, since SO_2 reduction appears to occur with good kinetics at Pt cathodes.

Whenever a given cathodic current density, i, can be achieved at a more positive electrode potential at an illuminated p-type semiconductor than at the conventional electrode, η is positive and finite. The extent to which i is obtained at a more positive potential is given the symbol E_V, and the power saved is $A(iE_V)$ (Figure 1), where A is the area of the electrode. It is worth noting that negative values of η are possible; an often encountered example is in the generation of H_2, stemming from the poor kinetics for H_2 evolution from unmodified semiconductor surfaces.[6] The maximum efficiency,

η_{max}, occurs at a particular current density, i_{opt} (Figure 1). The extent to which i_{opt} is obtained at an electrode potential positive of that of the conventional electrode is given the symbol E_V-(opt), and the power saved is $A(i_{opt}E_V(\text{opt}))$. The point on the current–voltage curve where η_{max} is realized is the analogue of the maximum power point for photovoltaic devices. A further complicating feature in photoelectrosynthesis is that the i_{opt} may not be optimum from the standpoint of current efficiency for the desired process or from the standpoint of desired rate of product generation.

If the optical source for a photoelectrosynthetic cell is the sun and the reason for the use of the photocathode is to save energy, η_{max} must likely exceed some minimum value. For large-scale electricity generation with photovoltaic cells driven by sunlight, the minimum useful efficiency for converting solar energy to electricity has been judged to be $\sim 10\%$.[7] It is likely that η_{max} would have to be much higher than 10% in order to offset the disadvantages associated with the intermittent solar insolation and the generation of a chemical over a large area.

In principle, redox reactions unique to semiconductor photoelectrodes can be found, and in such cases the value of η_{max} may be a less critical factor depending on the value of the chemical. For those cases where a unique reaction could be effected at the photoelectrode, controllable nonsolar optical sources could be viable, again depending on the value of the product. Redox reactions unique to a semiconductor electrode could occur for those situations where the redox-active species or the products from reaction interact strongly and specifically with the semiconductor surface. Such interactions would be expected for "inner-sphere" type electrode reactions where the redox reagent does become bonded to the electrode surface.

Experimental Section

Materials. Single-crystal B-doped, p-type Si (0.35 mm thick, 3–7 Ω cm, (100) face exposed) was obtained from Monsanto Co. Single-crystal p-WS_2 was generously provided by GTE laboratories and has been recently characterized as having a carrier concentration of $\sim 10^{18}$ cm^{-3}.[8] Single-crystal, Zn-doped ($\sim 10^{18}$ cm^{-3}) p-type InP (0.5–1.0 mm thick, (111) face exposed) was provided by Dr. G. Iseler of Lincoln Laboratories and has been previously characterized.[9] Single-crystal, Sn-doped ($\sim 10^{18}$ cm^{-3}), n-type InP (0.5–1.0 mm thick, (111) face exposed) was also provided by Dr. G. Iseler. Reagent grade P_2O_5, methylene blue, NaOH, $NaClO_4$, $AgNO_3$, I_2, KI, K_2PtCl_6, and 2-propanol were used as received from commercial sources. Purified grade $Na_2S_2O_4$ was obtained from Fisher Scientific Co. HPLC grade CH_3CN (Baker) was distilled over P_2O_5 before use and passed through neutral aluminum oxide (Woelm) which was dried under vacuum at 400 °C for 48 h. Electronic grade [n-Bu_4N]ClO_4 (Southwestern Analytical) was dried under vacuum at 80 °C for 24 h. Anhydrous SO_2 (Matheson) was used without further purification. Electronic grade HF (Allied) was used.

Electrode Preparation and Treatment. Ohmic contact to the back side of the Si was made by vapor deposition of Al followed by sintering at 723 K under N_2 for 5 min. The Al-plated surface was then lightly scratched and secured to a coiled Cu wire with conducting silver epoxy. The Cu-wire lead was passed through a 4-mm glass tube, and all surfaces were then sealed with Epoxy-Patch 1C white epoxy (Hysol Division, Dexter Corp.) so as to leave only the front surface ((100) face) exposed.

Just prior to use, the Si electrodes were first etched in concentrated HF for 60 s, rinsed with H_2O, and then placed in a solution of 15% NaOH in H_2O at 85 °C for 5–10 min followed by transfer without rinsing to a solution of 1% NaOH and 3.5% 2-propanol in H_2O also at 85 °C for 5–10 min to texture the (100) surface by revealing pyramids on the surface having (111) sides. The electrodes were then

(4) The power savings efficiency has been utilized in characterizing cells for the photoelectrolysis of H_2O: Heller, A. In "Proceedings of the 3rd Conference on Solar Energy Conversion and Storage", Aug 1982; p 63.

(5) Bockris, J. O.; Reddy, A. K. N. "Modern Electrochemistry"; Plenum Press: New York, 1970; Chapter 10.

(6) (a) Dominey, R. N.; Lewis, N. S.; Bruce, J. A.; Bookbinder, D. C.; Wrighton, M. S. *J. Am. Chem. Soc.* **1982**, *104*, 467. (b) Heller, A.; Vadimsky, R. G. *Phys. Rev. Lett.* **1981**, *46*, 1153. (c) Fan, F.-R. F.; Reichman, B.; Bard, A. J. *J. Am. Chem. Soc.* **1980**, *102*, 1488. (d) Abruna, H.; Bard, A. J. *Ibid.* **1981**, *103*, 6898.

(7) "Solar Photovoltaic Energy Conversion"; American Physical Society: New York, 1979.

(8) Baglio, J. A.; Calabrese, G. S.; Harrison, D. J.; Kamieniecki, E.; Ricco, A. J.; Wrighton, M. S.; Zoski, G. D. *J. Am. Chem. Soc.* **1983**, *105*, 2246.

(9) Dominey, R. N.; Lewis, N. S.; Wrighton, M. S. *J. Am. Chem. Soc.* **1981**, *103*, 1261.

rinsed with H_2O followed by CH_3CN and air-dried. This texturing procedure has been shown[10] to improve overall efficiencies over polished Si surfaces due to lower reflection losses.[11] We have found here that texturing also slightly improves the output parameters and that a much greater degree of reproducibility from electrode to electrode is obtained.

InP and WS_2 electrodes were fabricated in a manner similar to that used for p-Si. The ohmic contact to n-InP was established by rubbing Ga-In eutectic onto the back of the InP. An ohmic contact to p-InP was made by ultrasonic soldering (Sonobond Corp.) with a 1:1 In:Cd alloy followed by attachment of a Cu wire with In solder. Ohmic contact to p-WS_2 was made with Ag-epoxy. The InP electrodes were etched in $\sim$1 mM Br_2 in CH_3OH for 60 s at 25 °C prior to use. The p-WS_2 electrodes were not etched prior to use, since fresh surfaces are exposed in the fabrication procedure.[8]

Platinization of p-InP was accomplished by passing $\sim$2 × 10^{-2} C/cm^2 of cathodic charge at an illuminated ($\sim$40 mW/cm^2, 632.8 nm) p-InP electrode potentiostatted at 0.0 V vs. SCE in an O_2-free, aqueous 0.1 M $NaClO_4$ solution containing $\sim$1.5 mM K_2PtCl_6. Platinization of n-InP was accomplished at –0.2 V vs. SCE in the same solution and without illumination.

Equipment and Procedures. Cyclic voltammograms and steady-state current–voltage curves were obtained with a PAR Model 173 potentiostat equipped with a Model 175 programmer. Data were recorded on a Houston Instruments Model 2000 X-Y recorder or, for current vs. time plots, on a Hewlett-Packard strip chart recorder. For cyclic voltammograms a single-compartment cell was used with a standard three-electrode configuration with Pt, n-InP, p-Si, p-WS_2, or p-InP as a cathode, a Pt anode, and an Ag/Ag^+ reference electrode (a silver wire immersed in 0.01 M $AgNO_3$/0.1 M [n-Bu_4N]ClO_4/ CH_3CN at +0.35 V vs. SCE). Controlled-potential electrolyses were carried out in a two-compartment cell in which the Pt anode was isolated by an ultrafine glass frit.

Electrodes were illuminated with a beam-expanded 632.8-nm He-Ne laser (Aerotech Model LS5P) providing $\sim$40 mW/cm^2. Higher intensities were obtained with a beam-expanded argon ion laser (Spectra-Physics Model 164-03) tuned to 514.5 nm providing $\sim$1 W/cm^2 or a focused 300-W incandescent lamp providing $\sim$100 mW/cm^2. The laser intensity was varied with a photographic polarizing filter and monitored with use of a beam splitter and a Tektronix J16 radiometer equipped with a J6502 probe. The laser beam was generally masked to match the size of the electrode surface.

SO_2 gas was introduced by injection of measured quantities into sealed cells containing rigorously dry and O_2-free [n-Bu_4N]ClO_4/ CH_3CN in which the volume of N_2 or Ar over the solution was minimized. The approximate concentration of SO_2 in these solutions was determined by titration with standardized triiodide solutions.[12]

Methylene blue is known[13] to be specific for the oxidation of $S_2O_4^{2-}$ even in the presence of SO_3^{2-}, HSO_3^-, and $S_2O_3^{2-}$, which are known decomposition products of $S_2O_4^{2-}$.[13] Thus, we assayed $Na_2S_2O_4$ by titration of the samples dissolved in 50% by volume CH_3OH in 0.1 M $NaOH/H_2O$ with 1.0 mM aqueous methylene blue. The samples were titrated under N_2 or Ar to prevent decomposition of the $S_2O_4^{2-}$ by O_2/H_2O oxidation. Infrared measurements of KBr pellets of $Na_2S_2O_4$ were made on a Perkin-Elmer Model 180 spectrometer.

Results

a. Cyclic Voltammetry of SO_2 in Nonaqueous Solution. While the mechanism of the electrochemical reduction of SO_2 in nonaqueous media has been shown to be rather complex,[3] it is the general view that there is an initial one-electron reduction (eq 3), followed by one or more equilibrium reactions.
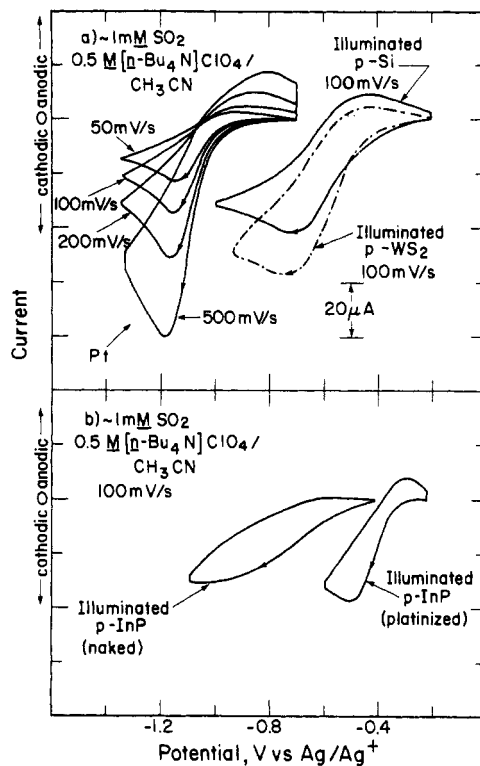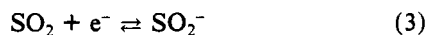
$$SO_2 + e^- \rightleftharpoons SO_2^- \qquad (3)$$

(10) (a) Bruce, J. A.; Wrighton, M. S. *J. Electroanal. Chem. Interfacial Electrochem.* **1981**, *122*, 93. (b) Bruce, J. A.; Wrighton, M. S. *Isr. J. Chem.* **1982**, *22*, 184.

(11) (a) Kern, W. *RCA Rev.* **1978**, *39*, 287. (b) Baraona, C.; Brandhorst, H. *Conf. Rec. IEEE Photovoltaic Spec. Conf.* **1975**, *11*, 44. (c) Restrepo, F.; Backus, C. E. *IEEE Trans. Electron Devices* **1976**, *23*, 1195.

(12) (a) Peters, D. G.; Hayes, J. M.; Hieftje, G. M. "Chemical Separations and Measurements"; W. B. Saunders: Philadelphia, PA, 1974; p 328. (b) Killer, F. C. A.; Underhill, K. E. *Analyst (London)* **1970**, *95*, 505.

(13) Rinker, R. G.; Gordon, T. P.; Mason, D. M.; Sakaida, R. R.; Corcoran, W. H. *J. Phys. Chem.* **1960**, *64*, 573.

Figure 2. Comparison of the cyclic voltammetry of $\sim$1 mM SO_2 solutions in 0.1 M [n-Bu_4N]ClO_4/CH_3CN at Pt and the various photocathodes illuminated at 632.8 nm ($\sim$40 mW/cm^2).

Of these follow-up reactions, the most important is the dimerization of SO_2^- to form $S_2O_4^{2-}$ (eq 4).

$$2SO_2^- \rightleftharpoons S_2O_4^{2-} \qquad (4)$$

Cyclic voltammetry of $\sim$1 mM $SO_2/N,N$-dimethylformamide solutions at Pt has been shown to give a quasi-reversible wave at $\sim$–1 V vs. SCE with the cathodic wave being attributed to the process represented by eq 3.[3a,b] Since p-type WS_2,[8] Si,[14] and InP[9] have been well characterized in CH_3CN/[n-Bu_4N]ClO_4 solutions by cyclic voltammetry, we chose to examine the photoelectrochemical reduction of SO_2 in this medium. The difference in cathodic current peak positions for a p-type photocathode and an inert metallic electrode such as Pt has been used[8,9,14] as one measure of the output photovoltage for the photocathode with respect to the $E°{'}$ of the particular solution couple used. Figure 2a shows our data for the reduction of SO_2 in $CH_3CN/0.1$ M [n-Bu_4N]ClO_4. A cathodic peak attributable to the one-electron reduction of SO_2 is seen at $\sim$–1.2 V vs. Ag/Ag^+ at Pt, while this peak occurs $\sim$500 mV more positive at illuminated ($\sim$40 mW/cm^2, 632.8 nm) p-type Si and p-WS_2 electrodes, consistent with expectations based on previous studies[8,14] of other redox couples at p-type Si and WS_2 in CH_3CN/[n-Bu_4N]ClO_4 in this potential regime.

The cyclic voltammetry of SO_2 at naked p-type InP can be seen in Figure 2b. In contrast to p-type Si and WS_2, the naked p-InP photocathode does not give the photovoltage ($\sim$800 mV) found for other redox couples in this potential regime.[9] This is possibly due to poor interfacial charge-transfer kinetics for reduction of SO_2 at p-InP and suggests a need for modification of the InP surface to improve the kinetics for SO_2 reduction.

Since there has been success in improving interfacial kinetics by deposition of Pt onto photoelectrode surfaces,[6,15] we take

(14) (a) Bocarsly, A. B.; Bookbinder, D. C.; Dominey, R. N.; Lewis, N. S.; Wrighton, M. S. *J. Am. Chem. Soc.* **1980**, *102*, 3683. (b) Bookbinder, D. C.; Lewis, N. S.; Bradley, M. G.; Bocarsly, A. B.; Wrighton, M. S. *Ibid.* **1979**, *101*, 7721.

this approach here. Further justification for the use of the platinization procedure comes from the fact that the Pt electrode appears to give a good cyclic voltammogram for the SO_2 (Figure 2a). Figure 2b shows the effect of electrochemical deposition of $\sim 5 \times 10^{-8}$ mol/cm^2 of Pt onto p-InP. The wave for the platinized photocathode is much sharper than that for the naked electrode, and the peak occurs at a significantly more positive potential than for the naked electrode. Thus, the platinized p-InP appears to give a photovoltage of ~ 700 mV with respect to Pt based on cathodic peak separation. This value is nearly that found for fast, reversible one-electron redox couples in the same potential regime.[9]

The deposition of Pt onto p-InP can clearly improve the performance of the p-InP with respect to the SO_2 reduction. Improvement in the response could be due either to inhibition of surface recombination of electron-hole pairs or improvement in the kinetics for the heterogeneous SO_2 reduction process or to a combination of these effects. We favor the conclusion that the kinetics for the reduction process are significantly improved. Support for this conclusion comes from a study of the cyclic voltammetry of SO_2 at n-type InP. For an n-type semiconductor, reduction processes are possible without illumination, since electrons are the majority charge carrier. Moreover, for sufficiently negative redox couples the n-type semiconductor should behave as a metallic electrode. Metallic behavior is expected for n-type InP as a cathode for SO_2 reduction since fast, one-electron redox couples respond reversibly in the dark for those redox couples having an $E^{\circ\prime}$ in the vicinity of the cathodic peak for SO_2 reduction at Pt.[16] However, n-InP gives very poor response with respect to SO_2 reduction. Platinization of the n-type InP by electrochemical reduction of $PtCl_6^{2-}$, as for p-InP, results in substantial improvement of the kinetics for SO_2 reduction in that the cathodic peak shifts from ~ -1.5 V vs. Ag/Ag$^+$ to ~ -1.2 V vs. Ag/Ag$^+$ upon platinization in a 100 mV/s cyclic voltammogram. The cathodic peak at platinized n-InP is at nearly the same potential as at a Pt electrode, not unexpectedly. Since the reduction of SO_2 on n-InP is a major carrier process, reaction is not influenced by recombination effects. Thus, the improvement in performance of InP for SO_2 reduction by platinization can be attributed in large part to the improvement in SO_2 reduction kinetics.

A final issue of concern in connection with the use of the platinized InP electrodes is whether the Pt forms a uniform Schottky barrier or an ohmic contact to the InP such that the interface energetics are dominated not by the InP/solvent/electrolyte but rather by the Pt/solvent/electrolyte. If the p-InP/Pt contact were an ohmic contact, there would be no photoeffects and the cathode would simply behave as a Pt cathode with the p-InP as an in-series circuit element having a certain resistance. Clearly, the platinized p-InP does give photoeffects; the photocathodic peak in Figure 2b is ~ 700 mV more positive than at Pt (Figure 2a). This rules out the possibility that a uniform ohmic contact is obtained by electrodeposition of Pt onto p-InP. If the p-InP/Pt formed a uniform Schottky barrier, then photoeffects should be observed, but the output photovoltage would be controlled by the p-InP/Pt interactions. Experimentally, this can be tested by determining the output photovoltage for different redox couples having differing values of $E^{\circ\prime}$. For example, naked p-InP shows an output photovoltage of ~ 800 mV with respect to N,N'-dimethyl-4,4'-bipyridinium, MV^{2+}, $E^{\circ}(MV^{2+/+}) = -0.45$ V vs. SCE, whereas a smaller photovoltage is realized for redox
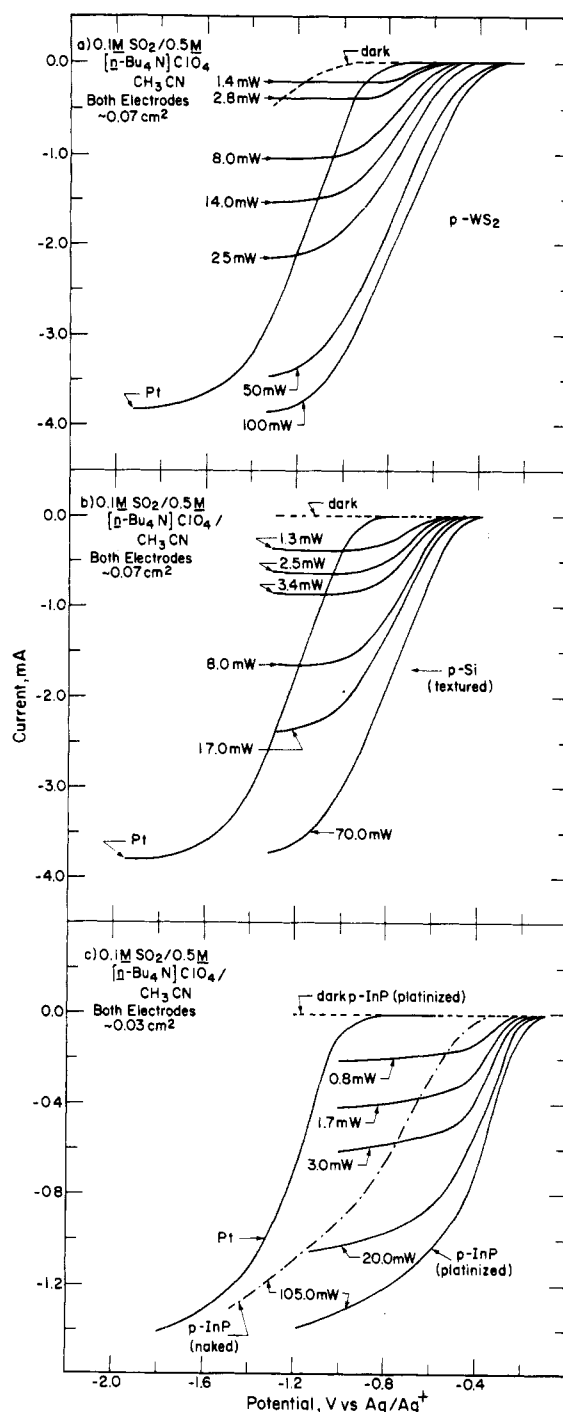

Figure 3. Steady-state current–voltage curves for Pt and the various photocathodes in 0.1 M SO_2/0.5 M [n-Bu$_4$N]ClO$_4$/CH$_3$CN at 10 mV/s. The illumination is at 514.5 nm at the indicated input power.

couples having a more positive $E^{\circ\prime}$, as measured by cyclic voltammetry. For the reduction of ferrocenium, $E^{\circ\prime} = +0.43$ V vs. SCE, we find that a naked p-InP photocathode gives ~ 200 mV of photovoltage, while the same electrode gives ~ 800 mV for reduction of MV^{2+}. Platinization of the p-InP gives the same results. The main point is that the platinized p-InP gives a photovoltage *dependent* on the electrochemical potential of the solution. A Schottky barrier p-InP/Pt electrode would give an electrochemical potential *independent* photovoltage. Thus, the data establish that the platinization of p-InP results in neither a uniform ohmic contact nor a uniform Schottky barrier. The deposited Pt does behave as a catalyst, as the results from n-InP show, without altering the interface energetics.

b. Steady-State Photocurrent–Voltage Curves for SO$_2$ Re-

(15) (a) Kautek, W.; Gobrecht, J.; Gerischer, H. *Ber. Bunsenges. Phys. Chem.* **1980**, *84*, 1034. (b) Nakato, Y.; Abe, K.; Tsubomura, H. *Ibid.* **1976**, *80*, 1002. (c) Nakato, Y.; Ohnishi, T.; Tsubomura, H. *Chem. Lett.* **1975**, 883.

(16) Dominey, R. N. Ph.D. Thesis, MIT, 1982. Dominey, R. N.; Stalder, C.; Wrighton, M. S., to be submitted for publication.

Table I. Representative Output Parameters for Reduction of SO_2 at p-Type Semiconducting Photocathodes in $CH_3CN/0.5$ M $[n\text{-}Bu_4N]ClO_4/0.1$ M SO_2

electrode	input optical pwr, mW (intens, mW/ cm²)[a]	$E_V(opt)$, mV[b]	$A(i_{opt}E_V(opt))$, mW[c]	η_{max}, %[d]	Φ_e[e]
p-WS₂	1.4 (20)	160	0.03	1.7	0.34
	2.8 (40)	160	0.05	1.7	0.34
	8.0 (114)	210	0.14	1.7	0.31
	14.0 (200)	210	0.22	1.6	0.27
	25.0 (357)	270	0.34	1.3	0.20
	50.0 (714)	320	0.91	1.7	0.16
	100.0 (1430)	400	1.4	1.4	0.09
textured p-Si	1.3 (19)	170	0.05	3.9	0.67
	2.5 (36)	220	0.11	4.4	0.62
	3.4 (49)	270	0.16	4.8	0.60
	8.0 (114)	280	0.35	4.4	0.50
	17.0 (243)	290	0.54	3.2	0.33
	70.0 (1000)	400	1.20	1.7	0.12
platinized p-InP	0.8 (27)	600	0.08	10.5	0.60
	1.7 (57)	660	0.18	10.8	0.57
	3.0 (100)	680	0.33	10.8	0.49
	20.0 (667)	680	0.56	2.8	0.12
	105.0 (3500)	760	0.76	0.7	0.03

[a] Incident 514.5-nm light provided by an Ar ion laser; cf. Figure 3 for current–voltage curves corresponding to these data. [b] Value of E_V where η_{max} is realized; cf. text. [c] Maximum power savings. [d] Optimum power savings efficiency defined as $A(i_{opt}E_V(opt))/$ (input optical power); cf. text. [e] Quantum yield for electron flow at limiting current density.

duction at p-Type Photocathodes. Figure 3 shows steady-state photocurrent–voltage curves for the reduction of SO_2 at p-type electrodes in 0.5 M $[n\text{-}Bu_4N]ClO_4/CH_3CN$ as a function of light intensity (514.5 nm). Also shown is the reduction of SO_2 at a Pt electrode of equivalent ($\pm 10\%$) geometrical area and configuration. Table I shows the data that were obtained from the curves in Figure 3. The cyclic voltammetry data in Figure 2 suggest that platinized p-InP should be the best candidate for efficient photoelectrolysis of $SO_2/CH_3CN/[n\text{-}Bu_4N]ClO_4$ solutions, and Table I indeed bears this out. Large photovoltages (>600 mV) and good quantum efficiencies (~0.6) combine to yield η_{max} for platinized p-InP, which exceeds 10%. Also shown in Figure 2 is a high light intensity curve for naked p-InP, to be compared with the curve at the same intensity for platinized p-InP. The difference here agrees with the results from the cyclic voltammetry experiments and again illustrates the consequences of kinetic sluggishness of naked InP with respect to reduction of SO_2 in $[n\text{-}Bu_4N]ClO_4/$ CH_3CN. Efficiencies for textured p-type Si are typically only ~4%, owing to the lower photovoltages obtained. Poor quantum yields and the low photovoltages for p-WS₂ result in the lowest efficiencies (~2%) of the three materials studied. The low efficiency for p-WS₂ is a result consistent with efficiencies for other redox reactions in the same potential regime and has been attributed to the consequences of junction breakdown at such negative potentials relative to the flat-band potential.[8]

Figure 3 and Table I include data as a function of light intensity. Note that the same limiting current density is obtained from the photocathodes as from Pt when the light intensity is sufficiently high. At the 0.1 M SO_2 concentration employed, there is a mass transport limitation on the current density at sufficiently negative potentials. Thus, the quantum yield for electron flow on the plateau of the photocurrent–voltage curve, Φ_e, declines when the current density approaches that associated with the mass transport limit. Only at the lower light intensities, <100 mW/cm², are good values for Φ_e obtained. In principle, higher SO_2 concentrations should allow the use of higher light intensity without diminution of Φ_e.
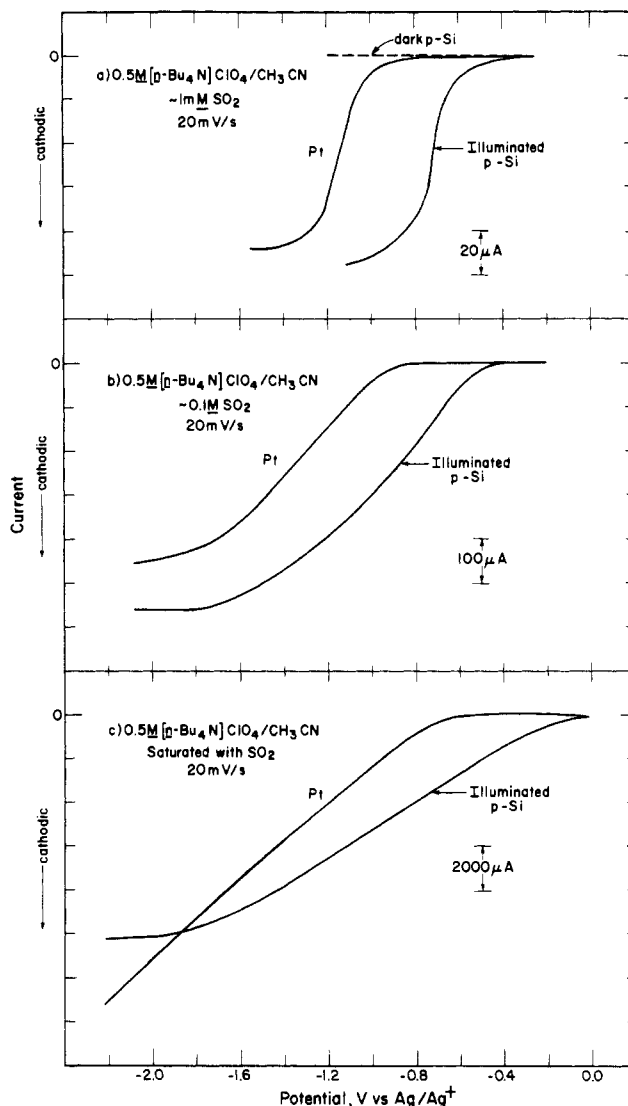
Figure 4. Steady-state current–voltage curves for Pt and textured p-type Si (illuminated, 514.5 nm, ~1 W/cm²) at varying SO_2 concentrations in 0.5 M $[n\text{-}Bu_4N]ClO_4/CH_3CN$ solutions. Both electrodes have the same area, ~0.1 cm².

Figure 4 shows steady-state current–voltage curves for Pt and illuminated (514.5 nm, ~2 W/cm²) p-Si cathodes as a function of SO_2 concentration. At ~1 mM SO_2 and 0.1 M SO_2 the current density is limited by mass transport for both Pt and illuminated p-Si. However, for the saturated SO_2 (>1.0 M) case the current density is not limited by mass transport in the potential regime examined. Rather, for the p-Si electrode kinetics and/or light intensity limit the current density. Similar results are found for p-WS₂ and platinized p-InP. Thus, it is apparent that SO_2 concentrations higher than those used for the experiments in Figure 3 will allow the use of higher light intensities. However, at very high light intensities electron–hole recombination at the surface of the photocathode and poor kinetics for SO_2 reduction can result in a decline in efficiency.

c. Preparative, Controlled-Potential Photoreduction of SO_2: Current Efficiency for $S_2O_4^{2-}$ and Durability of Photocathodes. We have been able to demonstrate that synthetically significant quantities of $Na_2S_2O_4$ can be prepared by photoelectrochemical reduction of SO_2 in $[n\text{-}Bu_4N]ClO_4/CH_3CN$ solutions at good current densities and with good current efficiency. The data are summarized in Table II. In a typical experiment, irradiation (~40 mW/cm², 632.8 nm) of the photocathode held at a fixed electrode potential in the cathode compartment of a two-compartment cell containing 100.0 mL of 0.1 M SO_2

Table II. Representative Data for the Production of $Na_2S_2O_4$ in 0.1 M SO_2/0.5 M [n-Bu_4N]ClO_4/CH_3CN Solutions

electrode[a] (area, cm^2)	potential vs. Ag/ Ag$^+$,[b] V	current dens, mA/ cm^2 [c]	t, h[d]	charge passed, C	$Na_2S_2O_4$ collected, mg[e]	η_i, %[f]
Pt (0.07)	−1.0	9.0	50	110	95	95
p-WS$_2$ (0.07)	−0.8	4.2	30	32	27	93
textured p-Si (0.07)	−0.8	6.0	80	120	104	96
textured p-Si (1.0)	−0.8	13.5	3	146	125	95
platinized p-InP (0.03)	−0.4	6.7	60	43	36	92

[a] Photocathodes were irradiated with ~40 mW/cm^2 of 632.8-nm light provided by a He–Ne laser except for the 1.0 cm^2 textured p-Si electrode, where an incandescent lamp providing >100 mW/cm^2 was employed. [b] Potential held in the cathode compartment of a two-compartment cell containing 100.0 mL of 0.1 M SO_2 in 0.5 M [n-Bu_4N]ClO_4/CH_3CN. [c] The measured photocurrent was constant, ±5%, in all experiments. [d] Time of cell operation. [e] Weight of the solid obtained upon addition of excess $NaClO_4$ to the catholyte. These amounts of $Na_2S_2O_4$ represent consumption of less than 10% of the total SO_2 originally present in the catholyte. [f] Current efficiency for $Na_2S_2O_4$ production with the assumption that the solid collected is 100% $Na_2S_2O_4$.

in 0.5 M [n-Bu_4N]ClO_4/CH_3CN results in a current density that is stable to within 5%. Upon completion of the electrolysis, addition of excess $NaClO_4$ caused formation of a fine, white precipitate, which is assayed to be >95% $Na_2S_2O_4$ by titration with methylene blue solution. The quantities of $Na_2S_2O_4$ collected represent consumption of less than 10% of the SO_2 originally present in the catholyte, consistent with little or no variation in current density. Further verification that the

powders are indeed $Na_2S_2O_4$ is obtained by noting the similarity of IR absorptions (400–4000 cm^{-1}) of the electrolysis samples and commercially available $Na_2S_2O_4$, although impurities in both prevent an exact spectral match.

Conclusions

Our data establish that illuminated p-type Si, WS$_2$, and InP electrodes can be used to lower the electrical energy requirement in the electrochemical generation of $Na_2S_2O_4$ from SO_2/CH_3CN/0.5 M [n-Bu_4N]ClO_4 solutions. Since $E°'$-(SO_2/$S_2O_4^{2-}$) in this medium is difficult to obtain, we must compare the photoelectrodes to an electrode, Pt, which is presumed to have rapid interfacial kinetics. Such a comparison is meaningful, since it gives a guide to the actual reduction in the electrical energy requirement for operation of a photoelectrosynthetic cell[1] compared to that for a conventional electrolytic cell. In any case, it is clear that platinized p-InP is the material of choice, as the power savings efficiency for conversion of 514.5-nm light is up to 11%. The durability of all of the photocathodes, particularly the platinized p-type InP, is good, and indeed the generation of synthetically significant quantities of $Na_2S_2O_4$ can be effected with >90% current efficiency. Others[6b] have shown that η_{max} exceeds 12% *solar efficiency* for the generation of H$_2$ from platinized p-InP. This suggests that the solar efficiency for $S_2O_4^{2-}$ production could be practically significant. However, the use of single-crystal InP electrode materials would likely be prohibitively expensive for practical applications.

Contribution from the Department of Chemistry,
Faculty of Science, Osaka City University, Sumiyoshi-Ku, Osaka 558, Japan

Studies of Formation of Zinc(II) Bromide, Iodide, and Thiocyanate Complexes in Methanol Using the Respective Ion-Selective Electrodes

HIDEKAZU DOE,* AKIO SHIBAGAKI, and TOYOKICHI KITAGAWA

The formation of ZnX_n^{2-n} (X$^-$ stands for Br$^-$, I$^-$, and NCS$^-$, respectively) complexes in methanol has been studied by X$^-$ ion measurements with Ag–AgX electrodes. All measurements have been made at an ionic strength of 0.05 M, adjusted with sodium and zinc perchlorates, and in a closed cell thermostated at 25.0 ● 0.1 °C. In the complexation of zinc(II) chloride in methanol, the cooperative phenomenon that the stepwise stability constant of a monochloride complex is smaller than that of a dichloride complex has already been reported. In the present studies, this same phenomenon has been also observed in the formation of bromide and iodide complexes of zinc(II). The degree of cooperativity steadily increases in going from the chloride to the iodide complex of zinc(II). On the other hand, the magnitude of stepwise stability constants of zinc(II) thiocyanate complexes is in the order generally found; that is, the constants decrease in going from the mono- to the tetrathiocyanate complex.

Introduction

Since many investigations of the equilibria of metal complexes have been made in aqueous solutions because of their great practical value, it is necessary to conduct these research studies in nonaqueous solvents so that one may understand the equilibrium constants theoretically and consistently. Generally, the stepwise stability constants of metal complexes, K_n, decrease with the increasing numerical value of n.[1] There are, however, some complexes that disobey the general trend for K_n values, and some of them have been already reported

elsewhere.[2,3] Then, as shown in some literature references,[4] zinc(II) halide complexes are typical of the cooperative phenomenon. In order to gain further insight into this phenomenon, we have studied the stabilities of ZnX_n^{2-n} complexes (X$^-$ stands for Br$^-$, I$^-$, and NCS$^-$, respectively) in methanol. Ex-

(1) King, E. L. *Inorg. Chem.* **1981**, *20*, 2350–2352.

(2) Doe, H.; Kitagawa, T. *Inorg. Chem.* **1982**, *21*, 2272–2276.
(3) Doe, H.; Matsui, M.; Shigematsu, T. *Bull. Inst. Chem. Res., Kyoto Univ.* **1980**, *58* (2), 154–163.
(4) (a) Ahrland, S.; Björk, N.-O. *Acta Chem. Scand., Ser. A* **1976**, *A30*, 256–269. (b) Ahrland, S.; Björk, N.-O.; Portanova, R. *Ibid.* **1976**, *A30*, 270–276. (c) Hoffman, H. *Pure Appl. Chem.* **1975**, *41*, 327–354. (d) Libuš, W.; Pastewski, R.; Sadowska, T. *J. Chem. Soc., Faraday Trans. 1* **1982**, *78*, 377–387.